# Pattern-Reconfigurable Printed Dipole Antenna for Wireless Communication Systems

Saber Dakhli[1,*], Jean Marie Floc'h[2], Ameni Mersani[3], and Hatem Rmili[4]

[1]*GeePs Laboratory, CNRS UMR-8507, CentraleSupélec, Université Paris-Saclay, F-91192 Gif-sur-Yvette, France*
[2]*IETR Laboratory, CNRS UMR-6164, INSA Rennes, Rennes, France*
[3]*ESPRIT School of Business, ZI. Chotrana II, Tunis P. O. Box 160, Tunisia*
[4]*Prince Sultan Defense Studies and Research Center (PSDSARC)*
*3075 Anas Ibn Malik Road, Riyadh, Saudi Arabia*

**ABSTRACT:** In this paper, a compact and reconfigurable radiation pattern dipole antenna based on the Yagi-Uda antenna principle and operating at 2.5 GHz is designed. Controlling the switching states of three loaded switches allows for pattern reconfigurability. Three modes can be chosen based on the results of the simulations and measurements. In the first mode M1, a directive-beam can be achieved by turning ON all the RF switches, and a measured peak gain of 6.7 dBi is obtained with a corresponding half-power beamwidth (HPBW) of 44°. In the second mode, only the director is required to enable a less directive beam. This allows for a larger HPBW of 62° and a lower peak gain of 5.47 dBi. Finally, by disabling the reflector and director in the third mode, M3, we get an omnidirectional radiation pattern around the $y$-axis with a maximum measured gain of 3.8 dBi. The comparison with other prior art antennas shows that the proposed reconfigurable antenna has compact size, high gain, and simple design, making the structure a good candidate for new wireless applications.

## 1. INTRODUCTION

With the fast improvement of wireless communications, many examples of pattern-reconfigurable (PR) antennas have been designed which allow better radiation performance and increasing coverage, quality, and capacity of signal propagation [1, 2]. Additionally, radiation pattern agility feature contributes to avoiding noisy environments, improving security, and saving energy by better directing the signal towards intended users, enhancing the performance of modern wireless communication systems. Phased-array antenna is a classic technique for tilting a beam [3, 4]. Controlling the feeding phase of radiation elements in the array antenna changes the direction of the radiation pattern.

Nevertheless, some disadvantages of phased-array antennas such as their large size, high cost, and complex design process would limit their use in communication systems. Many pattern-reconfigurable antennas have been proposed over the last few years in order to overcome the problems mentioned above. Many methods of pattern reconfigurability have been recently proposed in the literature. Yagi-Uda is used in [5] to realize different modes by controlling RF switching states in parasitic elements. The proposed antenna in [6] produced several reconfigurable beams by adjusting the amplitude and phase of each feeding point.

The radiation pattern of the antenna is achieved in [7] by controlling the phase of magnetic dipoles and using a two-element dipole array model. In [8], the antenna was controlled by a phase shifter and had two types of direction. It

was mounted on an artificial magnetic conductor that acted as a reflector. By shifting the states of the eight switches, eight pattern-reconfigurable modes could be created in [9]. In [10], a four-sector array was used, but the antenna's feeding network's circuits were too complicated to implement. The antenna in [11] achieved beam switching capability in the elevation plane by reconfiguring the parasitic striplines with 20 p-i-n diodes. A pattern-reconfigurable antenna described in [12] produced radiation patterns in both horizontal and vertical planes but was difficult to fabricate. In [13], a planar printed dipole antenna with reconfigurable radiation pattern properties was designed by combining two elementary dipoles. The agility of this antenna was provided by four PIN diodes. Depending on the switch state, the 2.56 GHz antenna can tilt its radiation pattern in two opposite directions.

All of the above designs have a common disadvantage of low antenna gain and large gain variation between different states, especially when some electronic switches are built into the antenna system. These problems make them less suitable for long-distance wireless communication.

This paper describes a PR antenna operating at 2.5 GHz which can exhibit both omnidirectional and directional radiation. The antenna can switch among three modes based on the states of the three switches.

By putting all RF switches in the "ON" state in the first mode, M1, a far beam with a half-power beamwidth (HPBW) of 44° and a measured peak gain of 6.7 dBi can be obtained. The second mode, M2, will be obtained by activating only one dipole and its director, resulting in a lower pattern (62°) and measured

---

\* Corresponding author: Saber Dakhli (saber.dakhli@centralesupelec.fr).
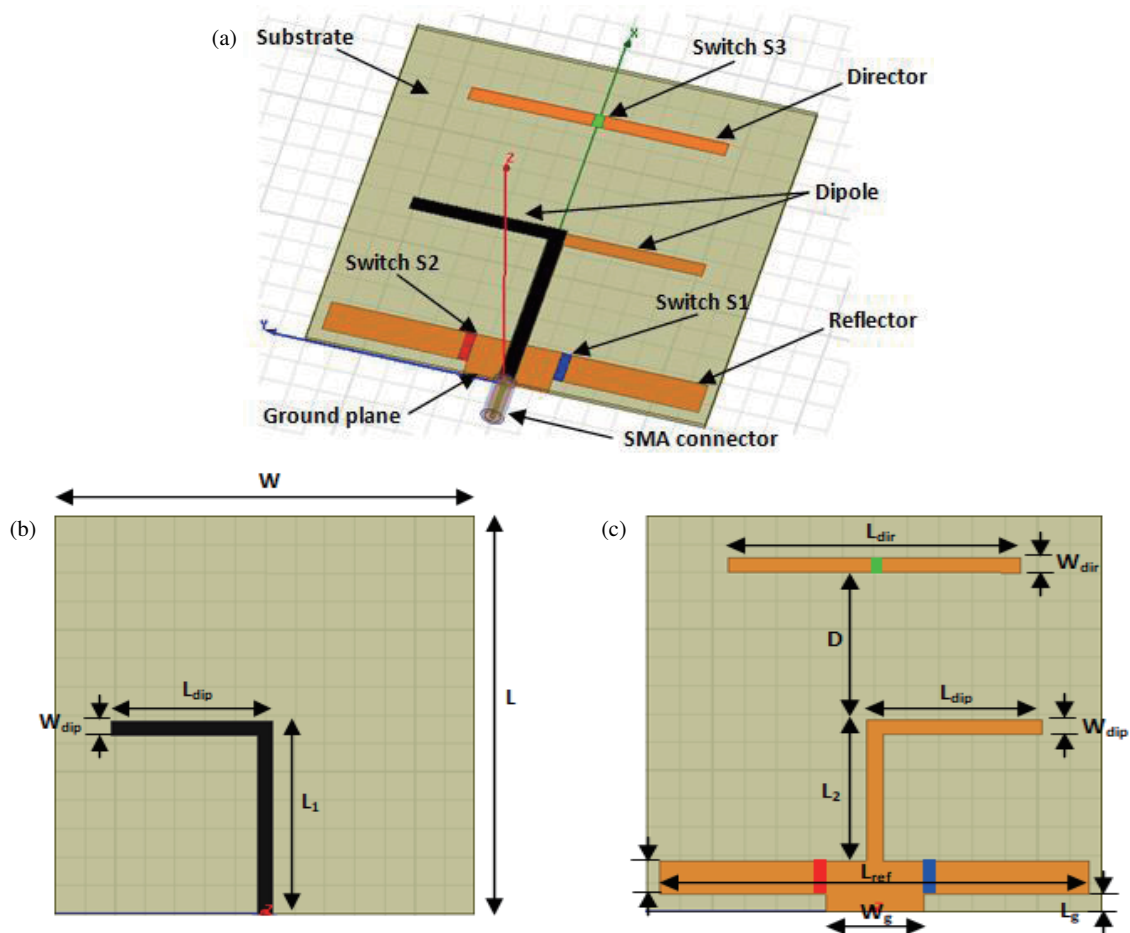
FIGURE 1. PR antenna: (a) HFSS design; (b) top view and (c) bottom view.

peak gain (5.47 dBi). By disabling the director and reflector, we were able to generate a third mode, M3. With this configuration, only the active dipole is radiating, resulting in an omnidirectional pattern with a gain of 3.8 dBi. The antenna has high gain and small gain difference in three modes, which is desirable for some medium/long-distance communication scenarios.

The manuscript is organized as follows. In Section 2, the proposed PR antenna topology, design, and fabrication details are presented. Then, in Section 3, the simulated and experimental performances of the PR antenna are discussed. Finally, Section 4 summarizes this work.

## 2. PR ANTENNA'S DESIGN METHODOLOGY

This section describes the methodology followed for the design of the PR antenna. First, we will present the antenna's design. Then, we will explain the principle of the chosen reconfigurability and the switching technique. Finally, we will present the fabricated prototypes.

### 2.1. PR Antenna's Design

The PR antenna's design process starts with a printed dipole. The proposed printed dipole was fabricated with a Rogers DuroidTM 5880 substrate with a thickness 0.8 mm, relative permittivity $\varepsilon_r = 2.2$, relative permeability $\mu_r = 1.0$, and loss

tangent $\delta = 0.0009$. ANSYS frequency structure simulator (HFSS) was used to simulate the structure. As shown in Fig. 1, the dipole has a three-layer structure. The dipole arm and associated microstrip positive lead are printed on top of the substrate. The second dipole arm and associated microstrip negative feeder are printed on its underside. The total length of both arms is $2 \times L_{dip} = 55$ mm.

The antenna impedance matching is affected by the distance $L_2$ between the arms and ground plane. The ground strip length was selected to be $L_{ref} = 60$ mm, slightly larger than $2 \times L_{dip}$, in order to act as a reflector, concentrating the radiated energy towards the frontside direction (positive $x$-axis). The ground strip's width (6 mm) and its feed-point portion (15 mm) were chosen to accommodate the SMA connector and facilitate manufacturing. An antenna operating at 2.5 GHz in the Industrial, Scientific, and Medical (ISM) band operates with an optimized distance $L_2 = 34$ mm between the dipole arms and the ground strip with no additional matching network. In order to increase the gain of the printed dipole in the positive $x$-axis direction, we added a metallic director to the ground side of the structure. The distance between the dipole arms and the director is close to $\lambda_0/4$ where $\lambda_0$ is the wavelength. Radiation must be concentrated in the front side direction by a director that is shorter than both arms of the dipole. The design details are presented

TABLE 1. Design parameters of the PR antenna.

| Parameters | $L$ | $W$ | $D$ | $L_{dip}$ | $W_{dip}$ | $L_1$ | $L_2$ | $L_{dir}$ | $W_{dir}$ | $L_{ref}$ | $W_{ref}$ | $L_g$ | $W_g$ |
|---|---|---|---|---|---|---|---|---|---|---|---|---|---|
| Value (mm) | 65 | 65 | 29 | 27.5 | 2 | 35 | 27 | 45 | 2 | 60 | 6 | 3 | 15 |

TABLE 2. Mode configurations by switches ON/OFF conditions.

| Mode | Configuration | Switch 1 | Switch 2 | Switch 3 |
|---|---|---|---|---|
| M1 | Dipole with activated reflector and director | ON | ON | ON |
| M2 | Dipole with activated reflector | ON | ON | OFF |
| M3 | Only dipole is activated | OFF | OFF | OFF |

in Fig. 1 and the parameters of the design are summarized in Table 1.

## 2.2. Principle of Reconfigurability

To achieve the reconfigurability of the proposed antenna, we have incorporated three switches into the structure. Each switch works in two operating states, "ON" (short-circuit) and "OFF" (open circuit). In Fig. 2, we explain the working principle of a single switch in states "ON" and 'OFF". In Fig. 1, two switches were placed in the reflector between the reflector and ground strip while the third one was placed in the middle of the director arm. The three radiation modes were chosen for the reconfigurable structure. The mode selection process is detailed in Table 2.
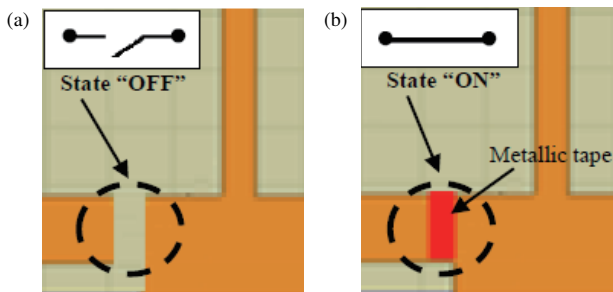


FIGURE 2. Working principle of the PR antenna: (a) States "OFF" (open circuit) and (b) States "ON" (short circuit).

## 2.3. Fabricated Prototypes

The optimized PR antenna was fabricated and characterized. Fig. 3 illustrates the prototypes of passive and the active printed dipoles with reflector and director.

Since the reflector plays an important role in forming the directive radiation, we have omitted mode 4, where the director is activated, and the reflector is deactivated, since it is without interest.

## 3. EXPERIMENTAL RESULTS AND DISCUSSION

In this section, we present simulated and measured results of impedance matching, surface current distribution, radiation patterns, gain, and efficiency for all modes.

The realized prototype was investigated by measuring its impedance matching over the frequency band 2–3 GHz and its radiation properties (gain, efficiency, and radiation patterns) by using an anechoic room (Satimo Starlab from the IETR Institute).

Simulated and measured results are in good agreement. The use of switches, as described above, allows the electronic control of the radiated beam at the operating frequency by activating or deactivating the reflector and/or director.

## 3.1. $S_{11}$ Parameter

A comparison of the measured and simulated reflection coefficients versus the frequency is given in Fig. 4, corresponding to the three modes M1, M2, and M3.

When Mode M1 is activated, the simulated frequency of the PR is around 2.5 GHz, while the measured one is around 2.48 GHz. The minor discrepancies between the results of the test and simulation are due to the effects of the switches. For Mode M2, simulation and measurement results are in good agreement at 2.5 GHz, as shown in Fig. 4(b).

In Fig. 4(c), we plot simulated and measured return losses versus frequency for Mode M3. In this case, the simulation operating frequency is 2.5 GHz (2.48 GHz for measurement), and the obtained matched bandwidth ($< 10$ dB) is 450.6 MHz (350 MHz for measurement). The mild discrepancies between the measured and simulated results are due in part to small fabrication inaccuracies and the presence of switches.

## 3.2. Current Distributions

To illustrate further the role of the switches in the antenna pattern modification, surface current distributions were simulated for the all studied modes as shown in Fig. 5. In the case of Mode M1, when the two switches are turned ON, both the reflector and director are activated as shown in Fig. 5(a). For Mode M2, the surface current distribution shown in Fig. 5(b) shows that the director is disabled, and only the dipole and reflector radiate in the $x$-direction. In the case of Mode M3, when the two switches are turned OFF, both the reflector and director are disabled, and only the dipole is active.

(a)



(b)                              (c)
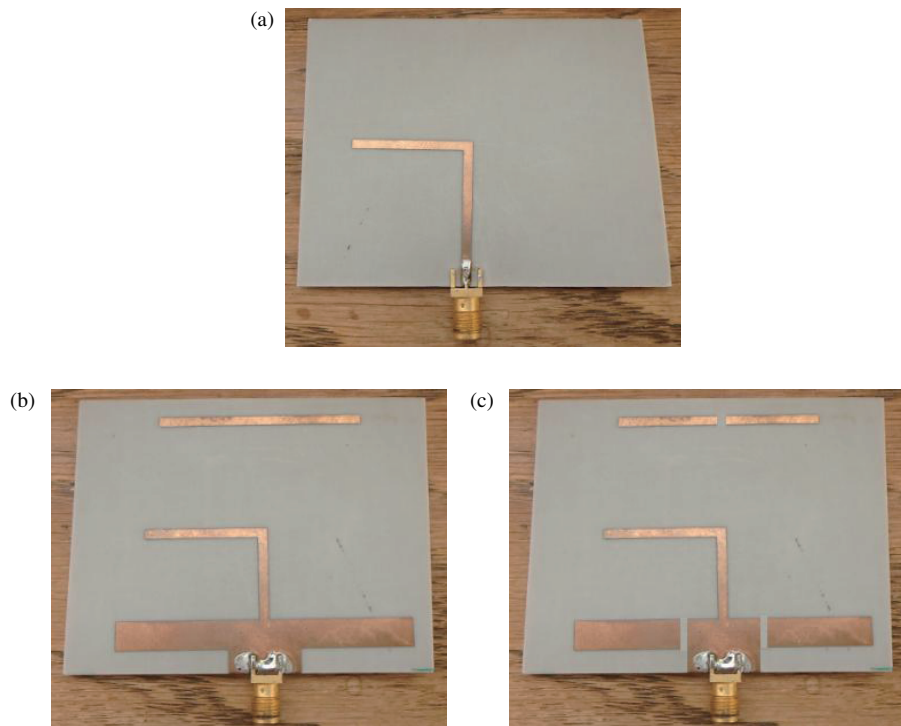


**FIGURE 3**. Photos of the PR antennas prototypes: (a) The passive structure top view, (b) back view, and (c) with the integrated open circuits.
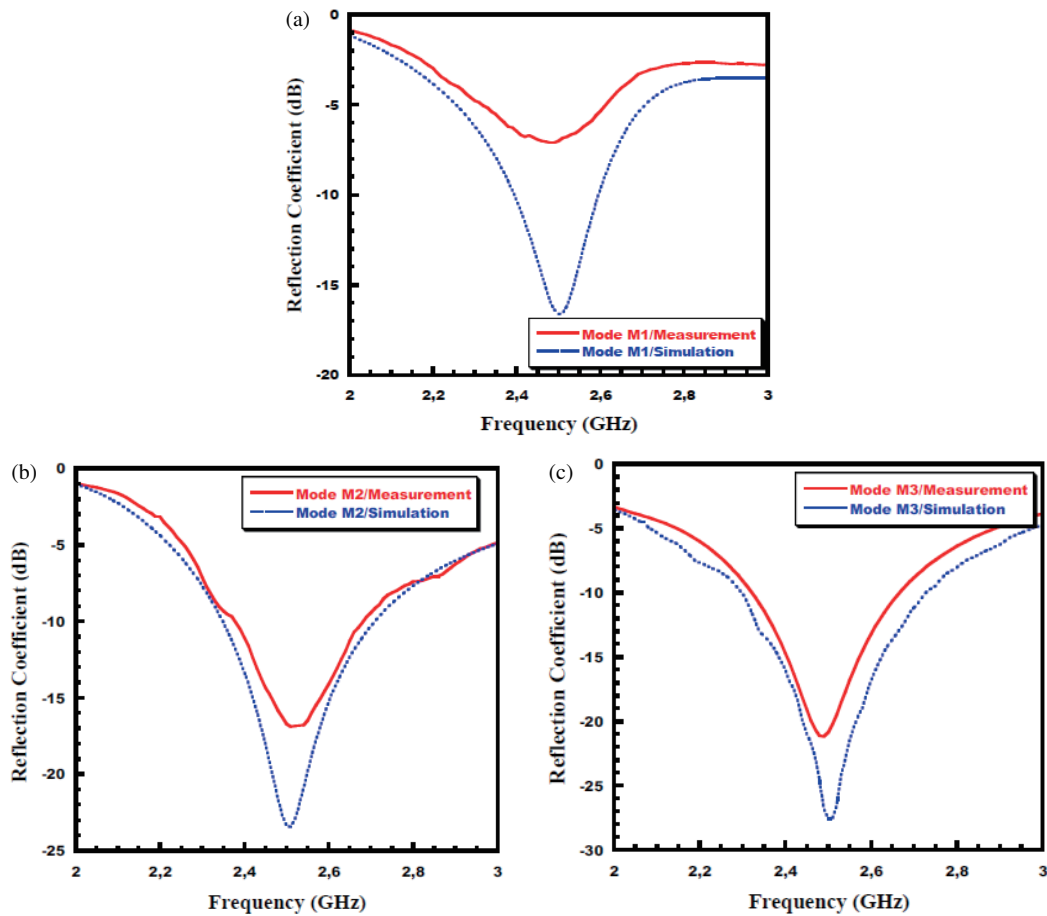


**FIGURE 4**. Simulated and measured reflection coefficients: (a) Mode M1, (b) Mode M2, and (c) Mode M3.
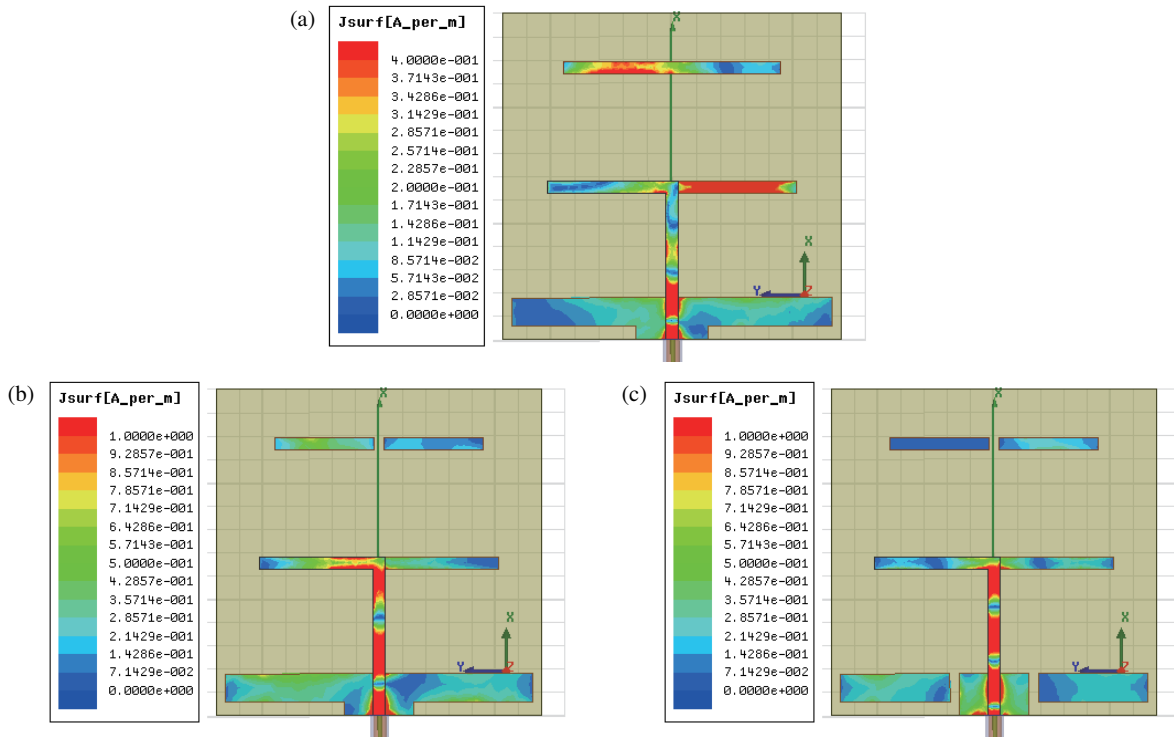
**FIGURE 5**. Simulated current distributions at the operating frequency 2.5 GHz: (a) Mode M1, (b) Mode M2, and (c) Mode M3.

**TABLE 3**. Summarized measured performances of the PR antenna for the three modes.

| Mode | Frequency operation (GHz) | HPBW (°) | Peak Gain (dBi) | Efficiency (%) |
|------|---------------------------|----------|-----------------|----------------|
| M1 | 2.5 | 44 | 6.7 | 68 |
| M2 | 2.52 | 62 | 5.47 | 80 |
| M3 | 2.48 | - | 3.8 | 88 |

**TABLE 4**. Performance comparison with antennas available in the state-of-the-art literature.

| Reference | Total size (mm) | Switch number | Mode number | Fr (GHz) | Maximum Gain (dBi) | Bandwidth (%) |
|-----------|-----------------|---------------|-------------|----------|--------------------|---------------|
| [15] | $80 \times 60 \times 0.8$ | 16 | 3 | 2.7 | 6.4 | 15.2 |
| [16] | $60 \times 30 \times 0.8$ | 12 | 3 | 9.3 | N/A | 6 |
| [17] | $67.4 \times 43 \times 0.76$ | 2 | 2 | 2.4 | 5 | 20.8 |
| [18] | $32 \times 62 \times 1.524$ | 4 | 3 | 2.03 | 5.8 | 2.46 |
| **This work** | $\mathbf{65 \times 65 \times 0.8}$ | **3** | **3** | **2.5** | **6.7** | **13.6** |

## 3.3. Radiation Patterns

The measured radiation patterns were obtained using the Satimo StarLab near-field measurement instrument. The radiation patterns for 2.48 GHz, 2.5 GHz, and 2.56 GHz are shown here because the antenna is intended for wireless communication applications. Figs. 6, 7, and 8 show the 3D simulation, 3D measurement, and the 2D measurement and simulation radiation patterns for these three modes, respectively.

The PR antenna presents a simulated peak gain of 7.64 dBi at the operating frequency 2.5 GHz (6.7 dBi for measurement) with a corresponding half-power beamwidth (HPBW) of 42° (44° for measurement) in Mode M1.

The 2D-radiation patterns demonstrated in Fig. 7 confirm this behavior predicted by simulations. Compared to Mode M1, the PR antenna has a less directive beam. The measured maximum gain is 5.47 dBi at the operating frequency of 2.52 GHz, while the simulated maximum gain is 5.69 dBi at the resonant frequency 2.5 GHz. In measurement, the half-power beamwidths are 62° and 65°, respectively.

Consequently, we obtain an omnidirectional radiation along the $y$-axis (Fig. 8). This is expected since the dipole's two arms are oriented along the $y$-axis. The maximum measured peak gain is 3.8 dBi (4.13 dBi for simulation.). The simulated radiation patterns in the $H$-plane ($OYZ$) at the operating frequency 2.5 GHz are plotted in Fig. 8(c).
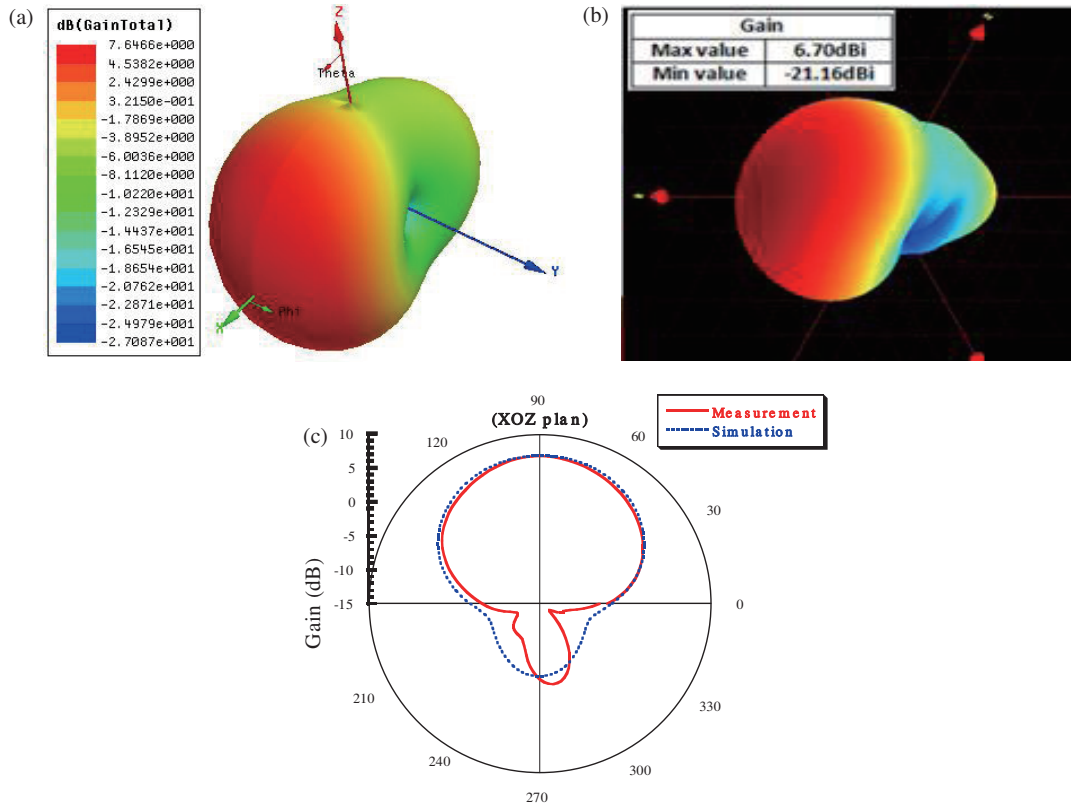
FIGURE 6. Radiation patterns for Mode M1. (a) 3D-simulation, (b) 3D-measurement (at 2.5 GHz), and (c) 2D-simulation and measurement (at 2.5 GHz).
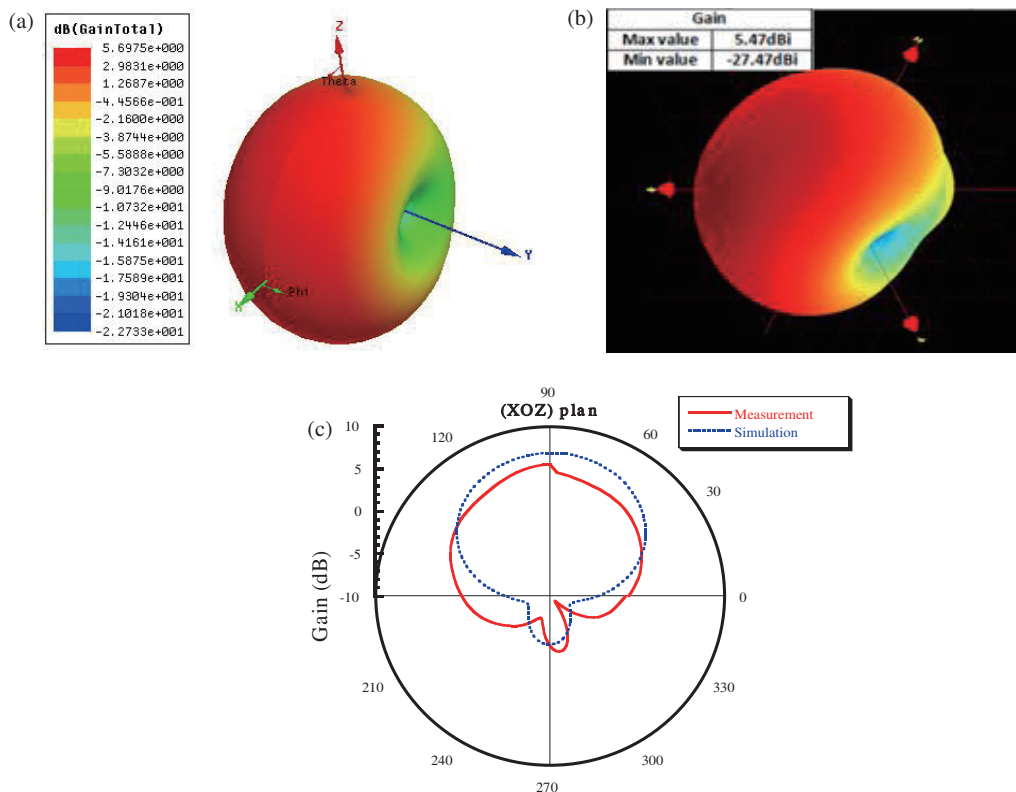


FIGURE 7. Radiation patterns for Mode M2. (a) 3D-simulation, (b) 3D-measurement (at 2.5 GHz), and (c) 2D-simulation and measurement (at 2.56 GHz).
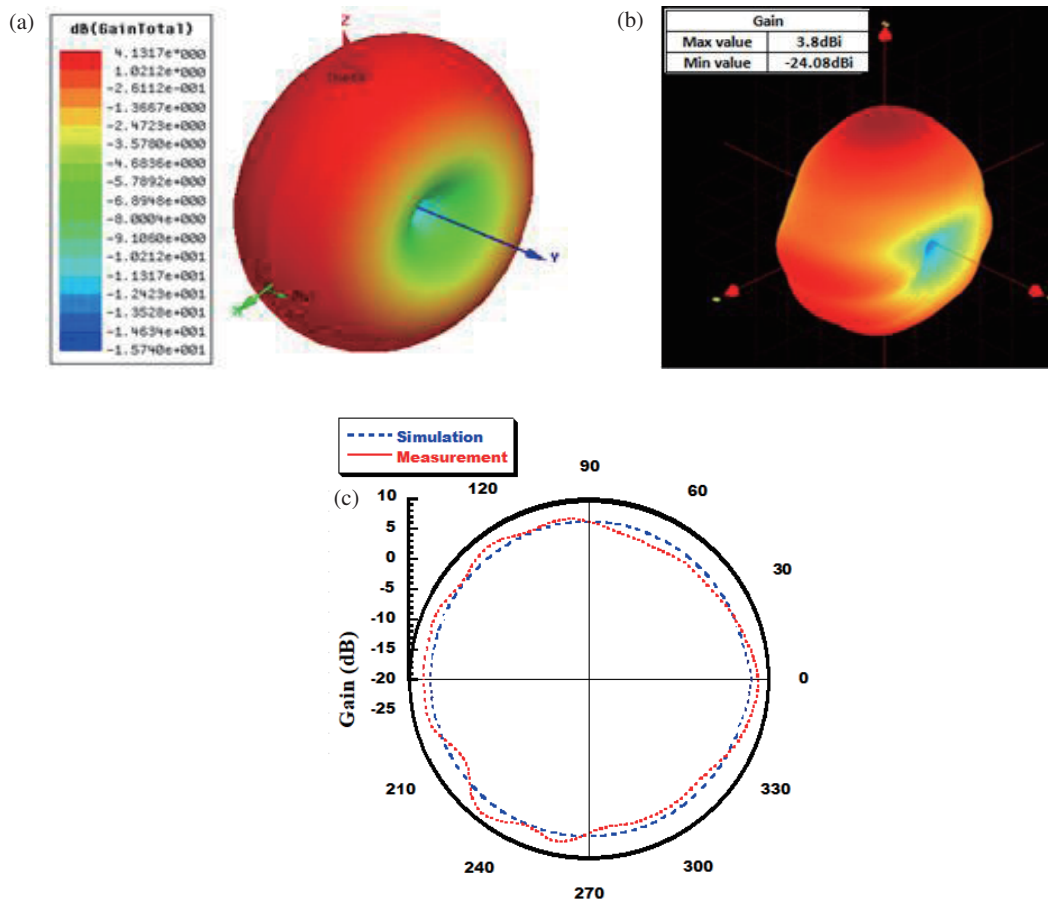
**FIGURE 8**. Radiation patterns for Mode M3. (a) 3D-simulation, (b) 3D-measurement (at 2.48 GHz), and (c) 2D-simulation and measurement (at 2.5 GHz).
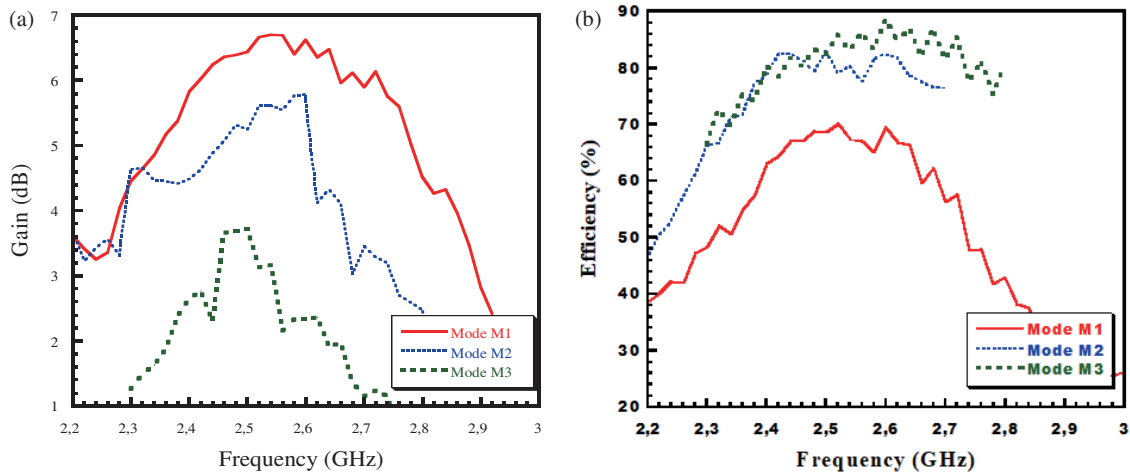


**FIGURE 9**. PR antenna (all modes): (a) Measured gain and (b) Measured efficiency.

## 3.4. Summary

It is clear from Table 3 that the antenna may display both a directive pattern (Modes M1 and M2) and an omnidirectional pattern depending on the switch states (Mode M3). It may switch simultaneously between a radiation pattern with directivity (Mode M1) and one with low directivity (Mode M2)

(since the director naturally improves the gain by better directing the radiation, was disabled).

According to Fig. 9(a) and Fig. 9(b), the measured results corresponding to Mode M1 showed maximum gains of 6.7 dBi and radiation efficiency of 68%. In the case of Mode M2, the measured peak realized gain values and radiation efficiency are respectively 5.47 dBi and 80%. Finally, the measured peak gain

and radiation efficiency are 3.8% and 88% for the omnidirectional mode, respectively. We can note that the gain variation is stable across the entire operating bandwidth for all the considered modes. Although Mode M1 is less efficient than the passive one, it still manages to achieve 68% efficiency at the operating frequency.

Table 3 provides a summary of the measured performance characteristics of the proposed PR antenna in the three studied modes in terms of frequency operation, HPBW, peak gain, and efficiency.

The profile, number of modes, frequency, peak gain, and bandwidth of our work are compared to some important parameters of existing PR antennas in Table 4. The proposed antenna indeed displays high gain, good efficiency, moderate bandwidth, and low profile.

## 4. CONCLUSION

A planar printed dipole antenna with reconfigurable radiation pattern properties has been proposed for wireless communication systems. The agility was ensured by using three switches. The antenna is designed to operate around 2,5 GHz. In Mode M1, 6.7 dBi of gain is achieved in a directive pattern and 5.47 dBi in a less directive pattern. When all switches are turned off, the antenna exhibits an omnidirectional pattern at 2.5 GHz with a maximum gain of 3.8 dBi. A frequency can be tuned by altering the distance between the reflectors and the dipole. The reflectors' size and shape can also be adjusted. This antenna has a greater gain and a less gain difference between states than other PR antennas. This antenna is an excellent choice for indoor wireless applications, such as ceiling-mounted antennas.

## REFERENCES

[1] Yang, X.-S., B.-Z. Wang, W. Wu, and S. Xiao, "Yagi patch antenna with dual-band and pattern reconfigurable characteristics," *IEEE Antennas and Wireless Propagation Letters*, Vol. 6, 168–171, 2007.

[2] Li, R., H. Yang, B. Liu, Y. Qin, and Y. Cui, "Theory and realization of a pattern-reconfigurable antenna based on two dipoles," *IEEE Antennas and Wireless Propagation Letters*, Vol. 17, No. 7, 1291–1295, 2018.

[3] Ke, Y.-H., L.-L. Yang, and J.-X. Chen, "Design of switchable dual-balun feeding structure for pattern-reconfigurable endfire antenna," *IEEE Antennas and Wireless Propagation Letters*, Vol. 20, No. 8, 1463–1467, 2021.

[4] Cheng, Y.-F., X. Ding, W. Shao, and B.-Z. Wang, "Planar wide-angle scanning phased array with pattern-reconfigurable windmill-shaped loop elements," *IEEE Transactions on Antennas and Propagation*, Vol. 65, No. 2, 932–936, Feb. 2017.

[5] Shi, Z., R. Zheng, J. Ding, and C. Guo, "A novel pattern-reconfigurable antenna using switched printed elements," *IEEE Antennas and Wireless Propagation Letters*, Vol. 11, 1100–1103, 2012.

[6] Chen, W.-H., F. L. Chen, N. Li, and Z. H. Feng, "Multi-feed reconfigurable pattern antenna implemented by switches," in *2005 IEEE Antennas and Propagation Society International Symposium*, Vol. 2, 400–403, 2005.

[7] Bai, Y.-Y., S. Xiao, C. Liu, X. Shuai, and B.-Z. Wang, "Design of pattern reconfigurable antennas based on a two-element dipole array model," *IEEE Transactions on Antennas and Propagation*, Vol. 61, No. 9, 4867–4871, Sep. 2013.

[8] Kim, K., K. Hwang, J. Ahn, and Y. Yoon, "Pattern reconfigurable antenna for wireless sensor network system," *Electronics Letters*, Vol. 48, No. 16, 984–985, 2012.

[9] Bai, Y.-Y., S. Xiao, M.-C. Tang, C. Liu, and B.-Z. Wang, "Pattern reconfigurable antenna with wide angle coverage," *Electronics Letters*, Vol. 47, No. 21, 1163–1164, 2011.

[10] Row, J.-S. and C.-W. Tsai, "Pattern reconfigurable antenna array with circular polarization," *IEEE Transactions on Antennas and Propagation*, Vol. 64, No. 4, 1525–1530, Apr. 2016.

[11] Chen, S.-L., P.-Y. Qin, W. Lin, and Y. J. Guo, "Pattern-reconfigurable antenna with five switchable beams in elevation plane," *IEEE Antennas and Wireless Propagation Letters*, Vol. 17, No. 3, 454–457, Mar. 2018.

[12] Hossain, M. A., I. Bahceci, and B. A. Cetiner, "Parasitic layer-based radiation pattern reconfigurable antenna for 5G communications," *IEEE Transactions on Antennas and Propagation*, Vol. 65, No. 12, 6444–6452, Dec. 2017.

[13] Ben Trad, I., J. M. Floc'h, H. Rmili, M. Drissi, and F. Choubani, "A planar reconfigurable radiation pattern dipole antenna with reflectors and directors for wireless communication applications," *International Journal of Antennas and Propagation*, Vol. 2014, No. 1, 593259, Jan. 2014.

[14] Floc'h, J.-M. and H. Rmili, "Design of multiband printed dipole antennas using parasitic elements," *Microwave and Optical Technology Letters*, Vol. 48, No. 8, 1639–1645, Aug. 2006.

[15] Ren, J., X. Yang, J. Yin, and Y. Yin, "A novel antenna with reconfigurable patterns using H-shaped structures," *IEEE Antennas and Wireless Propagation Letters*, Vol. 14, 915–918, 2015.

[16] Yang, X.-S., B.-Z. Wang, W. Wu, and S. Xiao, "Yagi patch antenna with dual-band and pattern reconfigurable characteristics," *IEEE Antennas and Wireless Propagation Letters*, Vol. 6, 168–171, 2007.

[17] Li, R., H. Yang, B. Liu, Y. Qin, and Y. Cui, "Theory and realization of a pattern-reconfigurable antenna based on two dipoles," *IEEE Antennas and Wireless Propagation Letters*, Vol. 17, No. 7, 1291–1295, Jul. 2018.

[18] Ke, Y.-H., L.-L. Yang, and J.-X. Chen, "Design of switchable dual-balun feeding structure for pattern-reconfigurable endfire antenna," *IEEE Antennas and Wireless Propagation Letters*, Vol. 20, No. 8, 1463–1467, 2021.